Matched-Pair Comparison of ^{18}F-DCFPyL PET/CT and ^{18}F-PSMA-1007 PET/CT in 240 Prostate Cancer Patients: Interreader Agreement and Lesion Detection Rate of Suspected Lesions

Maurits Wondergem, Friso M. van der Zant, Wouter A.M. Broos, Remco J.J. Knol

Department of Nuclear Medicine, Noordwest Ziekenhuisgroep, Alkmaar, The Netherlands

Over 20 different prostate-specific membrane antigen (PSMA)–targeting radiopharmaceuticals for both imaging and therapy have been synthesized. Although variability in biodistribution and affinity for binding to the PSMA receptor is known to exist between different PSMA-targeting radiopharmaceuticals, little is known about the clinical implications of this variability. Therefore, this study analyzed differences in interreader agreement and detection rate between 2 regularly used ^{18}F-labeled PSMA receptor–targeting radiopharmaceuticals: ^{18}F-DCFPyL and ^{18}F-PSMA-1007. **Methods:** One hundred twenty consecutive patients scanned with ^{18}F-PSMA-1007 were match-paired with 120 patients scanned with ^{18}F-DCFPyL. All 240 PET/CT scans were reviewed by 2 readers and scored according to the criteria of the PSMA Reporting and Data System. Interreader agreement and the detection rate for suspected lesions were scored for different anatomic locations such as the prostate, prostatic fossa, lymph nodes, and bone. **Results:** Great equality was found between ^{18}F-DCFPyL and ^{18}F-PSMA-1007; however, some clinically relevant and statistically significant differences were observed. ^{18}F-PSMA-1007 detected suspected prostatic or prostatic fossa lesions in a higher proportion of patients and especially in the subcohort scanned for biochemical recurrence. ^{18}F-DCFPyL and ^{18}F-PSMA-1007 showed an equal ability to detect suspected lymph nodes, although interreader agreement for ^{18}F-DCFPyL was higher. ^{18}F-DCFPyL showed fewer equivocal skeletal lesions and higher interreader agreement on skeletal lesions. Most of the equivocal lesions found with ^{18}F-PSMA-1007 at least were determined to be of nonmetastatic origin. **Conclusion:** Clinically relevant differences, which may account for diagnostic dilemmas, were observed between ^{18}F-DCFPyL and ^{18}F-PSMA-1007. Those findings encourage further studies, as they may have consequences for selection of the proper PSMA-targeting radiopharmaceutical.

Key Words: prostate cancer; PSMA; ^{18}F-DCFPyL; ^{18}F-PSMA-1007; PET/CT

J Nucl Med 2021; 62:1422–1429
DOI: 10.2967/jnumed.120.258574

In recent years, prostate-specific membrane antigen (PSMA) receptor PET/CT has rapidly evolved as a cornerstone in prostate cancer imaging. PSMA PET/CT outperforms other imaging modalities because of its superior sensitivity and specificity, although sensitivity for lymph node metastases has been found to be moderate in prospective trials (*1–5*). The better diagnostic characteristics account for better treatment selection in both primary staging and biochemical recurrence. The ability to detect small metastases, for example, may benefit patients with oligometastatic disease, offering them treatment options with a chance of cure or survival benefits (*6,7*), although scientific underpinning of the latter is needed (*8*). The additional value of PSMA PET/CT during follow-up of systemic treatment, including androgen deprivation therapy and chemotherapy, in the palliative phase of the disease also needs to be clarified.

Because of the success of PSMA PET/CT, the number of different radiopharmaceuticals targeting the PSMA receptor has increased significantly (*9*). Although most early publications on the clinical use of PSMA PET/CT reported on findings with ^{68}Ga-labeled radiopharmaceuticals, later publication also gave attention to ^{18}F-labeled radiopharmaceuticals. Positrons emitted by ^{18}F decay have lower kinetic energy than those emitted by ^{68}Ga, resulting in a higher resolution in PET images acquired using ^{18}F tracers. Furthermore, the 110-min half-life of ^{18}F, compared with 68 min for ^{68}Ga, enables imaging at later time points without significant deterioration of image quality or the need to administer higher doses. This point is of clinical importance since PSMA tracer kinetics show that the tracer accumulates in prostate cancer cells over time whereas the background activity decreases (*10–14*). Although over 20 different PSMA-targeting radiopharmaceuticals for both imaging and therapy have been synthesized, only a few are used in common clinical practice.

Variability in biodistribution and affinity for binding to the PSMA receptor is known to exist between the different PSMA-targeting radiopharmaceuticals, but little is known about the clinical implications of this variability (*15,16*). This lack is reflected in recent EAU guidelines that do not discriminate between different PSMA-targeted radiopharmaceuticals for imaging of prostate cancer (https://uroweb.org/guideline/prostate-cancer/). To investigate whether these differences are clinically important and interfere with the reproducibility of scan outcomes and lesion detection, this study analyzed—in a large matched-pair cohort of 240 patients—interreader agreement and detection rate for suspected lesions using 2 common ^{18}F-labeled PSMA receptor–targeting radiopharmaceuticals: 2-(3-(1-carboxy-5-[(6-^{18}F-fluoro-pyridine-3-carbonyl)-amino]-pentyl)-ureido)-pentanedioic acid (^{18}F-DCFPyL) and (3*S*,10*S*,14*S*)-1-(4-(((*S*)-4-carboxy-2-((*S*)-4-carboxy-2-(6-^{18}F-fluoronicotinamido)butanamido)butanamido)methyl)phenyl)-3-

Received Oct. 20, 2020; revision accepted Jan. 13, 2021.
For correspondence or reprints, contact Maurits Wondergem (m.wondergem@nki.nl).
Published online February 5, 2021.
COPYRIGHT © 2021 by the Society of Nuclear Medicine and Molecular Imaging.

(naphthalen-2-ylmethyl)-1,4,12-trioxo-2,5,11,13-tetraazahexadecane-10,14,16-tricarboxylic acid (^{18}F-PSMA-1007). Known differences between these 2 radiopharmaceuticals that may interfere with scan readability include differences in excretion pathways and bone marrow uptake (*15,16*). Renal excretion of ^{18}F-DCFPyL results in high activity in the urinary tract, which may interfere with detection of lesions near the ureters and urinary bladder, whereas activity in the urinary tract is usually less for ^{18}F-PSMA-1007 because biliary excretion is the most important excretion pathway. Physiologic bone marrow uptake is commonly higher for ^{18}F-PSMA-1007 and may interfere with detection of bone metastases.

MATERIALS AND METHODS

Patient Population

This study retrospectively included 120 consecutive patients imaged between April 2, 2019, and June 20, 2019, with ^{18}F-PSMA-1007 PET/CT for primary staging, biochemical recurrence, or follow-up of systemic treatment of prostate cancer. In addition, 120 patients who were imaged between November 3, 2016, and March 21, 2019, with ^{18}F-DCFPyL were extracted from a prospectively maintained database of 813 patients scanned with ^{18}F-DCFPyL. To allow for a fair comparison of these 2 cohorts, they were matched on the basis of disease stage (primary staging, biochemical recurrence, or follow-up of treatment for castration-resistant prostate cancer); prostate-specific antigen (PSA) level at the time of PET/CT (PSA difference of <10% between 2 patients); and, in cases of biochemical recurrence, previous treatment (prostatectomy, lymph node dissection, external radiation therapy, or brachytherapy).

Besides the standard PSMA PET/CT acquired for clinical indications, no additional measurements or actions affecting the patient were performed. The study was approved by the local scientific board, and the need to receive approval from the local ethical committee was waived because the study did not fall within the scope of the Dutch Medical Research Involving Human Subjects Act (section 1.b; February 26, 1998). Additionally, as a standard procedure in our department, all included patients gave written consent to use of their anonymized data for scientific purposes.

Image Acquisition

^{18}F-DCFPyL and ^{18}F-PSMA-1007 were synthesized by an on-site cyclotron facility. PET images were acquired on a Biograph-16 TruePoint PET/CT scanner (Siemens Healthcare) at 120 min after injection of ^{18}F-DCFPyL (mean of 319 MBq and range of 231–367 MBq, depending on body mass) or 90 min after injection of ^{18}F-PSMA-1007 (mean of 324 MBq and range of 239–363 MBq, depending on body mass). Images were acquired from the inguinal region to the base of the skull (5 min per bed position). Data were reconstructed using an iterative ordered-subset expectation maximization 3-dimensional algorithm using 4 iterations, 16 subsets, and a 5-mm gaussian filter. The image matrix size was 256 × 256, pixel spacing was 2.67 × 2.67 mm, and slice thickness was 4 mm. For attenuation correction, a radiocontrast-enhanced CT scan (110 mAs at 110–130 kV) was typically acquired. Collimation was 16 × 1.2 mm; pitch, 0.95; slice thickness, 4 mm; and matrix size, 512 × 512. The resulting voxel sizes were 1.37 × 1.37 mm for CT images for attenuation correction and 0.98 × 0.98 mm for diagnostic CT images.

Data Acquisition

All 240 PET/CT scans were reevaluated by 2 nuclear medicine physicians with ample experience in reading both ^{18}F-DCFPyL and ^{18}F-PSMA-1007 PET/CT (each reader had >300 readings of both ^{18}F-DCFPyL and ^{18}F-PSMA-1007). The readers had access to limited patient data, including clinical indication for PSMA PET/CT, PSA level at time of PSMA PET/CT, Gleason score, TNM stage if known before PSMA PET/CT, and previous treatments. Readers were masked to all other data, including the used radiopharmaceutical.

The scan outcome was scored for different anatomic localizations, including prostate or prostatic fossa, inguinal lymph nodes, pelvic lymph nodes (N1 nodes, according to the TNM system in the eighth edition of the *AJCC Cancer Staging System*), abdominal lymph nodes, thoracic lymph nodes, axillary lymph nodes, cervical lymph nodes, pelvic bones, vertebral bones, thoracic bones (costae, sternum, clavicula, and scapulae), bones of the extremities, and other suspected lesions. The scans were read using the criteria of the PSMA Reporting and Data System (RADS) (*17*). For each anatomic localization, scan outcomes were entered in a database. Only the lesions with the highest score or highest likelihood of malignancy according to the reading system were recorded. If one or both readers found only equivocal lesions outside the prostate or prostatic bed, the true nature of the equivocal finding was retrospectively determined using data from histopathologic biopsies, imaging at follow-up, or PSA response to therapy. Definitive proof of nonmetastasized disease included, first, histopathologic findings excluding metastasized disease and, second, complete biochemical response after local therapies including prostatectomy, lymphadenectomy, or radiation therapy without or after discontinuation of androgen deprivation therapy and without local therapy of the equivocal findings. Definitive proof of metastasized disease included concordant findings on MRI, progression of lesions on follow-up PSMA PET/CT, or PSA response to targeted therapy that was administered because of equivocal findings.

Statistical Analysis

The Mann–Whitney *U* test was used to test for differences between ^{18}F-DCFPyL and ^{18}F-PSMA-1007 outcomes. Interreader agreement was measured by calculating the weighted Cohen κ and the percentage of agreement. As conventionally done, agreement was categorized as poor, fair, moderate, good, or very good, reflecting agreement of 0%–19%, 20%–39%, 40%–59%, 60%–79%, and 80%–100%, respectively. Weighted κ is highly dependent on the proportion of positive scan results; therefore, a low weighted κ may reflect good or even very good agreement when proportions of positivity are relatively low (?<0.2) or high (?>0.8) (*18*). For calculation of differences between ^{18}F-DCFPyL and ^{18}F-PSMA-1007 and agreement between readers, some subcategories of the PSMA RADS reading system were merged since some subdivisions barely have clinical impact: 1a, 1b, and 2 (benign and likely benign); 3a, 3b, 3c, and 3d (equivocal); and 4 and 5 (likely malignant and malignant). Pie plots were constructed for outcomes that showed relevant differences. All analyses were performed using the Statistical Package for Social Sciences (SPSS Statistics, version 25.0; IBM).

RESULTS

In total, 240 ^{18}F-PSMA PET/CT scans—120 ^{18}F-DCFPyL and 120 ^{18}F-PSMA-1007—were included in the study (Table 1). Commonly found differences between ^{18}F-DCFPyL and ^{18}F-PSMA-1007 uptake are shown in Figure 1.

Prostate and Prostatic Fossa

For the prostate and prostatic fossa, interreader agreement was very good for ^{18}F-DCFPyL and good for ^{18}F-PSMA-1007 (Fig. 2). Both readers found significantly more suspected prostate lesions with ^{18}F-PSMA-1007 using the PSMA RADS criteria (Table 2; Supplemental Fig. 1; supplemental materials are available at http://jnm.snmjournals.org). Categorization of the cohort according to disease stage shows statistical differences for detection of

TABLE 1
Patient Characteristics

Characteristic	^{18}F-DCFPyL	^{18}F-PSMA-1007
All patients		
n	120	120
PSA (μg/mL)	11.6 (0.1–558)	12.0 (0.1–577)
Primary staging		
n	69	69
PSA (μg/mL)	14.8 (3.2–558)	14.7 (2.4–577)
Gleason score*		
≤7a	17	8
≥7b	51	58
Unknown	1	4
T stage†		
T1	23	15
T2	25	27
T3	16	22
T4	0	4
Unknown	5	1
Androgen deprivation therapy	0	0
Biochemical recurrence		
n	21	21
PSA (μg/mL)	2.4 (0.4–7.9)	2.4 (0.4–7.8)
Previous therapy		
Prostatectomy	7	7
Radiation therapy	12	12
Brachytherapy	2	2
Androgen deprivation therapy‡	1	2
Follow-up systemic treatment		
n	30	30
PSA (μg/mL)	24.8 (0.1–385.0)	26.3 (0.1–369.0)
Androgen deprivation therapy	30	30

*$P = 0.402$ (Mann–Whitney *U* test),
†$P = 0.009$ (Mann–Whitney *U* test).
‡Only temporarily after radiation therapy with curative intent.
Qualitative data are number; continuous data are median followed by range in parentheses.

suspected prostate lesions by both readers for patients with biochemical recurrence only (Table 3).

Lymph Nodes

Interreader agreement for lymph nodes was in general good to very good for both ^{18}F-DCFPyL and ^{18}F-PSMA-1007. However, a consistently lower agreement, for both weighted κ and percentage of agreement, was found for detection of suspected pelvic lymph nodes and lymph nodes at any localization with ^{18}F-PSMA-1007. No statistically significant differences were found between ^{18}F-DCFPyL and ^{18}F-PSMA-1007 for detection of suspected lymph nodes (Table 2). However, with ^{18}F-PSMA-1007 more lymph nodes showed low-level uptake comparable to blood-pool activity, matching score 1b or 2 (benign or likely benign) (Supplemental Fig. 2). For most anatomic regions, significantly more lymph nodes with low uptake were found with ^{18}F-PSMA-1007 than with ^{18}F-DCFPyL ($P < 0.0005$–0.037).

Bone Lesions

Regarding suspected bone lesions, almost perfect interreader agreement was found at all localizations for ^{18}F-DCFPyL. For ^{18}F-PSMA-1007, however, consistently lower agreement (both weighted κ and percentage of agreement) was found for lesions in the thoracic region and whole skeleton and to a lesser extent for suspected bone lesions in the pelvis (Fig. 2). Both readers scored a significantly greater number of equivocal bone lesions in the thoracic region with ^{18}F-PSMA-1007 (14%–33% and 3%–4% for ^{18}F-PSMA-1007 and ^{18}F-DCFPyL, respectively) at the expense of the number of scans without bone lesions (44%–62% for ^{18}F-PSMA-1007 and 76%–78% for ^{18}F-DCFPyL). The same was found for bone lesions at any localization (equivocal: 14%–33% for ^{18}F-PSMA-1007 and 3%–4% for ^{18}F-DCFPyL; no bone lesions: 30%–44% for PSMA 1007 and 64%–66% for ^{18}F-DCFPyL) (Table 2; Fig. 3). Reader 2 also scored a significantly greater number of equivocal pelvic lesions ($P = 0.027$), whereas for reader 1 no statistically significant difference was found ($P = 0.053$). Categorization according to disease stage shows that a significantly greater number of equivocal lesions were found with ^{18}F-PSMA-1007 at primary staging and biochemical recurrence ($P = 0.001$ and 0.003, respectively), also at the expense of the number of patients without bone lesions (Table 3).

Visceral Lesions

Visceral lesions were found in 3% of patients by both readers for both ^{18}F-PSMA-1007 and ^{18}F-DCFPyL, whereas equivocal lesions were found in 5%–6% of patients with ^{18}F-DCFPyL and 8% of patients with ^{18}F-PSMA-1007 (Table 2). No statistical differences were found between ^{18}F-PSMA-1007 and ^{18}F-DCFPyL for detection of other lesions. All patients who showed suspected lesions at other locations had extensive metastasized disease in lymph nodes and skeleton.

Equivocal Bone Lesions

Three patients scanned with ^{18}F-DCFPyL (1 primary staging, 1 biochemical recurrence, and 1 therapy follow-up) and 26 scanned with ^{18}F-PSMA-1007 (18 primary staging, 6 biochemical recurrence, and 2 therapy follow-up) had equivocal bone lesions as the only indication of possible metastasized disease. Clinical follow-up of these patients showed definite proof of nonmetastasized disease in 0 and 16 (62%) patients scanned with ^{18}F-DCFPyL and ^{18}F-PSMA-1007, respectively, whereas 1 (33%) and 2 (8%) showed proof of metastasized disease, and no conclusive follow-up was present in 2 (67%) and 8 (31%). Three patients had histopathologic verification of equivocal bone lesions on ^{18}F-PSMA-1007; none of these lesions were proven to be malignant (Fig. 4). Histopathology showed benign etiologies: aspecific necrosis, an aspecific lytic bone lesion with reactive changes, and normal bone tissue.

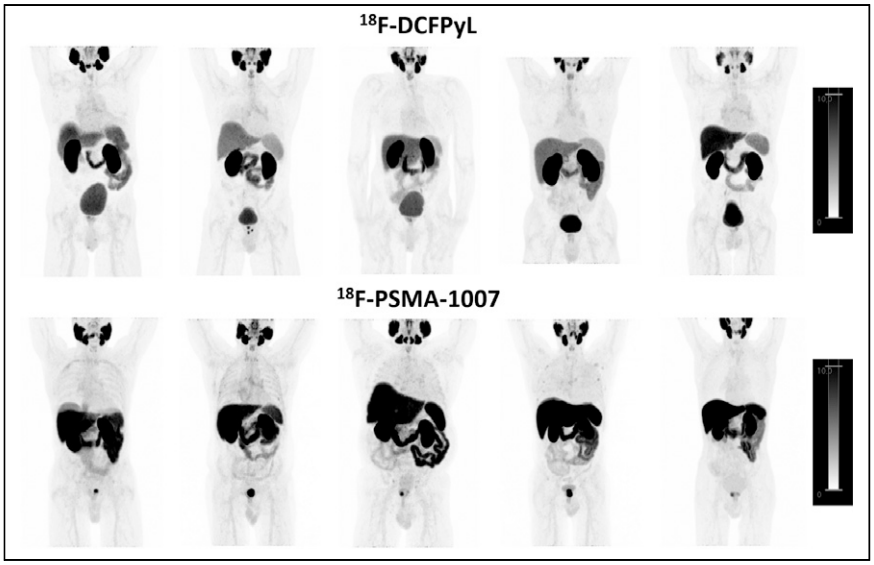

FIGURE 1. Distribution of ^{18}F-DCFPyL and ^{18}F-PSMA-1007 in patients imaged for primary screening of high-risk prostate cancer, all scored as negative for bone and lymph node metastases by 2 experienced readers. Maximum-intensity-projection images are scaled to SUV-body weight of 0.0–10.0. Lower physiologic ^{18}F-DCFPyL uptake is observed in liver, spleen, and bone marrow. Lower ^{18}F-DCFPyL uptake is observed in primary prostate tumor. Low ^{18}F-PSMA-1007 activity is seen in urinary tract and trachea. ^{18}F-PSMA-1007 uptake in skeleton is heterogeneous between patients; no uptake to diffuse uptake is observed in bone marrow, and variable patterns of irregular ^{18}F-PSMA-1007 uptake are observed in ribs of several patients. Higher ^{18}F-PSMA-1007 activity in bile ducts and gallbladder is not appreciated because of scaling.

DISCUSSION

Although great equality was found between ^{18}F-DCFPyL and ^{18}F-PSMA-1007 for interreader agreement and for detection of suspected prostate cancer lesions, there were 2 differences that may be of clinical relevance.

The first was in the prostatic region; identification of lesions in this region is of particular clinical importance for patients with biochemical recurrence. The subanalysis according to clinical stage showed that, especially in this category of patients, ^{18}F-PSMA-1007 detected significantly more suspected lesions than ^{18}F-DCFPyL, although the number of patients in this category was limited (n = 21). That finding could be the result of the lower urinary secretion of this radiopharmaceutical, allowing for better characterization of intraprostatic lesions or lesions in the prostatic fossa after prostatectomy.

Second, equivocal bone lesions were found more frequently with ^{18}F-PSMA-1007, resulting in lower interreader agreement. The greatest difference between readers was in the classification of rib uptake. Both readers acknowledged high uptake in the ribs in many patients scanned with ^{18}F-PSMA-1007. Reader 1 interpreted this uptake as probably benign (PSMA RADS 2) in a larger proportion of patients than did reader 2, who scored a larger proportion as equivocal (PSMA RADS 3a–3d). Reader 1 argued that the absence of lesions at other sites in the skeleton made bone metastases in the ribs unlikely; however, reader 2 scored these rib lesions as equivocal based purely on the increased activity in the ribs. Reader 2 argued that solitary bone metastases in the ribs are encountered in prostate cancer patients, although (as far as is known today) normally not as frequently as is observed with ^{18}F-PSMA-1007. The PSMA RADS reading criteria allow for interpretation differences, since no hard cutoffs to classify tracer uptake are given. Although allowing for differences in interpretation is scientifically less desirable, such differences continuously exist in clinical practice, and these data therefore reflect the present discussion around this topic in daily practice. Findings of equivocal PSMA-avid bone lesions may be clinically relevant and account for diagnostic dilemmas, such as when there are no other metastatic lesions or when the equivocal findings distinguish between oligo- and polymetastatic disease. In these cases, the true nature of these equivocal findings may alter patients' management and indicate the need for further diagnostic procedures.

Given that the study was retrospective, it had the drawback that histopathologic confirmation was lacking for almost all lesions. However, clinical follow-up of patients with equivocal bone lesions as the only indication of possible metastasized disease showed that in most patients (at least 16/24) with these abnormalities on ^{18}F-PSMA-1007, metastasized disease could be excluded. However, metastasized disease was proven in only 2 of 26 patients. These results indicate that equivocal bone findings with ^{18}F-PSMA-1007 PET/CT are of little clinical value and should not cause withholding of treatment options with curative intent.

As another drawback of the study, because ^{18}F-DCFPyL and ^{18}F-PSMA-1007 were compared between patients, some findings may be attributable to differences between cohorts rather than to differences between radiopharmaceuticals. However, to diminish these influences, we used 2 large cohorts comprising matched-pair

	Total cohort			
	DCFPyL		PSMA-1007	
	Weighted κ	Agreement (%)	Weighted κ	Agreement (%)
Prostate	0.925	95	0.738	90
Lymph nodes				
Inguinal	0.265	96	0.746	99
Pelvis	0.915	95	0.841	89
Abdomen	0.848	93	0.833	93
Mediastinum	0.852	96	0.673	94
Axillae	1.000	100	1.000	100
Neck	0.773	95	0.952	98
Whole body	0.916	94	0.825	88
Bone				
Pelvis	0.895	95	0.823	86
Spine	0.893	95	0.912	93
Thorax	0.925	95	0.706	74
Extremities	1.000	100	0.847	94
Whole skeleton	0.868	93	0.659	70

FIGURE 2. Interreader agreement reflected by weighted Cohen κ and by percentage for both ^{18}F-DCFPyL and ^{18}F-PSMA-1007. Dark green = very good agreement; light green = good agreement; orange = moderate agreement.

TABLE 2
Detection Rates of Suspected Lesions and Equivocal Lesions and Testing of Equality for Detection of Suspected Lesions Between ^{18}F-DCFPyL and ^{18}F-PSMA-1007 for Total Cohort

		Reader 1					Reader 2				
		^{18}F-DCFPyL		^{18}F-PSMA-1007			^{18}F-DCFPyL		^{18}F-PSMA-1007		
General site	Specific site	Suspected malignant	Equivocal	Suspected malignant	Equivocal	*P*	Suspected malignant	Equivocal	Suspected malignant	Equivocal	*P*
Prostate		86 (72)	4 (3)	98 (82)	7 (6)	0.045*	86 (72)	5 (4)	102 (85)	1 (1)	0.015*
Lymph nodes	Inguinal	4 (3)	0 (0)	2 (2)	0 (0)	0.409	4 (3)	0 (0)	1 (1)	2 (2)	0.984
	Pelvis	52 (43)	2 (2)	55 (46)	4 (3)	0.409	52 (43)	2 (2)	55 (46)	5 (4)	0.460
	Abdomen	36 (30)	0 (0)	31 (26)	0 (0)	0.473	41 (34)	2 (2)	34 (28)	2 (2)	0.331
	Mediastinum	12 (10)	0 (0)	7 (6)	4 (3)	0.760	13 (11)	4 (3)	10 (8)	1 (1)	0.332
	Axillae	6 (5)	0 (0)	1 (1)	0 (0)	0.056	6 (5)	0 (0)	1 (1)	0 (0)	0.056
	Neck	12 (10)	0 (0)	11 (9)	1 (1)	0.983	18 (15)	0 (0)	11 (9)	1 (1)	0.231
	Whole body	52 (43)	2 (2)	56 (47)	5 (4)	0.463	55 (46)	4 (3)	58 (48)	6 (5)	0.691
Bone	Pelvis	32 (27)	2 (2)	44 (37)	5 (4)	0.053	32 (27)	0 (0)	40 (33)	13 (11)	0.027*
	Spine	28 (23)	2 (2)	34 (28)	4 (3)	0.215	26 (22)	1 (1)	34 (28)	10 (8)	0.060
	Thorax	23 (19)	4 (3)	29 (24)	17 (14)	0.015*	24 (20)	5 (4)	28 (23)	40 (33)	<0.001*
	Extremities	22 (18)	0 (0)	18 (15)	4 (3)	0.929	22 (18)	0 (0)	18 (15)	4 (3)	0.929
	Whole skeleton	40 (33)	4 (3)	50 (42)	17 (14)	0.009*	36 (30)	5 (4)	44 (37)	40 (33)	<0.001*
Other	Lung	1 (1)	4 (3)	1 (1)	7 (6)	0.389	1 (1)	6 (5)	2 (2)	6 (5)	0.800
	Liver	1 (1)	0 (0)	2 (2)	1 (1)	0.312	0 (0)	1 (1)	2 (2)	1 (1)	0.318
	Funiculus	0 (0)	2 (2)	0 (0)	0 (1)	0.156	2 (2)	0 (0)	0 (0)	0 (0)	0.800
	Adrenals	1 (1)	0 (0)	1 (1)	1 (1)	0.559	0 (0)	0 (0)	0 (0)	0 (0)	1.000
	Pleural	0 (0)	0 (0)	0 (0)	1 (1)	0.317	0 (0)	0 (0)	0 (0)	1 (1)	0.317
	Thyroid	0 (0)	0 (0)	0 (0)	0 (0)	1.000	0 (0)	0 (0)	0 (0)	1 (1)	0.317
	All other	3 (3)	6 (5)	4 (3)	10 (8)	0.270	3 (3)	7 (6)	4 (3)	9 (8)	0.513

*Statistically significant ($P < 0.05$; Mann–Whitney U test).
Data are number followed by percentage in parentheses. Suspected malignant PSMA is RADS 4 and 5; equivocal PSMA is RADS 3a, 3b, 3c, and 3d.

TABLE 3

Detection Rates of Suspected Lesions and Equivocal Lesions and Testing of Equality for Detection of Suspected Lesions Between ^{18}F-DCFPyL and ^{18}F-PSMA-1007 According to Primary Staging, Biochemical Recurrence, and Follow-up of Systemic Therapies

		Primary staging (n = 69)					BCR (n = 21)					Follow-up (n = 30)				
		^{18}F-DCFPyL		^{18}F-PSMA-1007			^{18}F-DCFPyL		^{18}F-PSMA-1007			^{18}F-DCFPyL		^{18}F-PSMA-1007		
Reader	Site	SM	Eq.	SM	Eq.	P	SM	Eq.	SM	Eq.	P	SM	Eq.	SM	Eq.	P
1	Prostate	66 (96)	2 (3)	67 (97)	2 (3)	0.669	6 (29)	0 (0)	13 (62)	3 (14)	0.007*	14 (47)	2 (7)	9 (30)	2 (7)	0.186
	Lymph nodes	24 (35)	1 (1)	27 (39)	4 (6)	0.393	11 (52)	1 (5)	9 (43)	1 (5)	0.532	17 (57)	0 (0)	20 (67)	0 (0)	0.430
	Whole skeleton	17 (25)	1 (1)	20 (29)	11 (16)	0.065	2 (10)	1 (5)	6 (29)	5 (24)	0.013*	20 (67)	1 (3)	24 (80)	1 (3)	0.234
2	Prostate	67 (97)	2 (3)	68 (99)	1 (1)	0.572	6 (29)	1 (5)	13 (62)	0 (0)	0.029*	13 (43)	2 (7)	21 (70)	0 (0)	0.059
	Lymph nodes	25 (36)	4 (6)	28 (41)	4 (6)	0.595	11 (52)	0 (0)	7 (33)	1 (5)	0.285	19 (63)	0 (0)	22 (73)	1 (3)	0.356
	Whole skeleton	15 (22)	2 (3)	15 (22)	27 (39)	0.001*	3 (14)	2 (10)	7 (33)	9 (43)	0.003*	18 (60)	1 (3)	22 (73)	4 (13)	0.154

*Statistically significant ($P < 0.05$; Mann–Whitney U test).

BCR = biochemical recurrence; SM = suspected malignant; Eq. = equivocal.

Data are number followed by percentage in parentheses. Suspected malignant PSMA is RADS 4 and 5; equivocal PSMA is RADS 3a, 3b, 3c, and 3d.

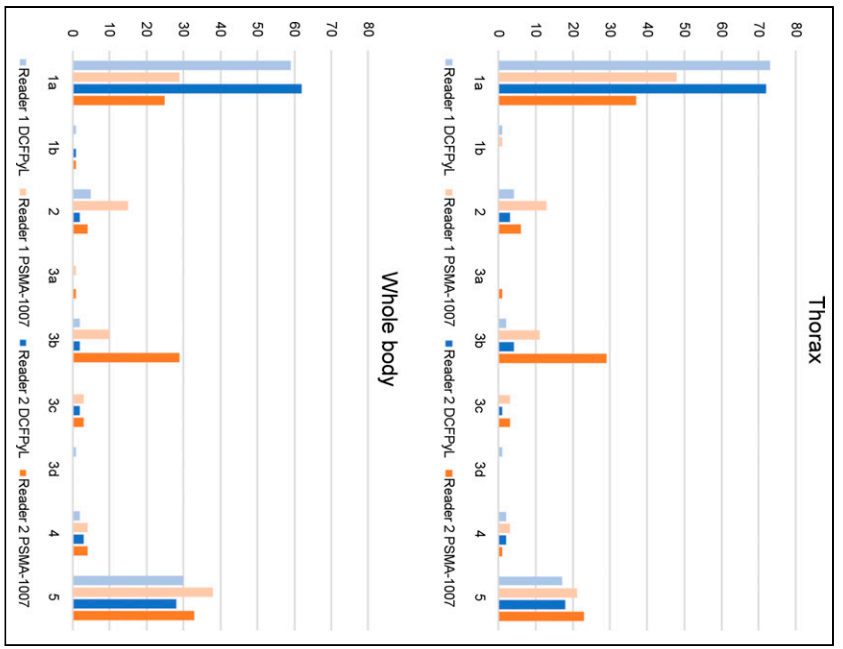

FIGURE 3. Bar graph for bone lesions in thorax and whole body. For ^{18}F-PSMA-1007, both readers scored statistically significantly greater number of equivocal lesions (3a, 3b, 3c, or 3 d) and fewer benign lesions (1a, 1b, and 2).

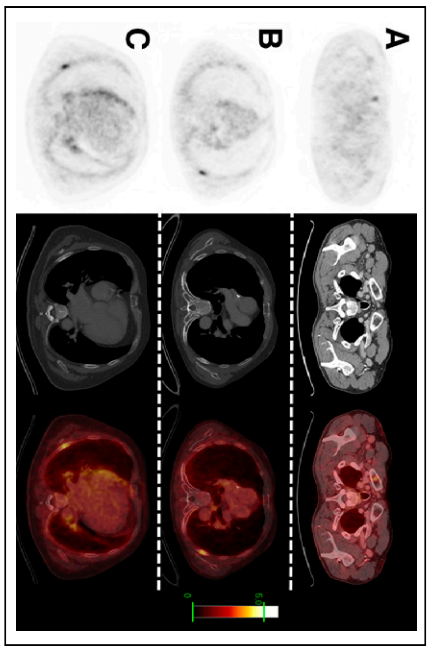

FIGURE 4. Equivocal bone lesions in right clavicula (A) and ribs (B and C) of clinical relevance for primary staging on ^{18}F-PSMA-1007 PET/CT. Tumor characteristics were cT3a, Gleason score of 7, and initial PSA of 15.2 ng/mL in A; cT2, Gleason score of 8, and initial PSA of 8.0 ng/mL in B; and cT3a, Gleason score of 6, and initial PSA of 3.7 ng/mL in C. Additional MRI could not exclude bone metastasis in A; no further imaging was performed in B and C. Histopathologic biopsy revealed no malignancy in any of these 3 patients: aspecific necrosis was found in A, aspecific lytic bone lesion with reactive changes in B, and normal bone tissue in C. Ultimately, all 3 patients were staged N0M0.

patients. Unfortunately, the databases were not large enough to enable pairing by all potentially relevant clinical characteristics that may interfere with the pretest likelihood of detecting suspected lesions. Matching of PSA was done instead of matching of Gleason score or T stage, since there are indications that ^{18}F-PSMA-PET/CT positivity for metastases is best predicted by the serum PSA value (*19*).

The findings in this study are in line with findings by Dietlein et al. in an intrapatient comparison of ^{18}F-PSMA-1007 with ^{18}F-DCFPyL, ^{68}Ga-PSMA-11, or ^{18}F-JK-PSMA-7 (*20*). In a cohort of 27 patients, an improved characterization of prostate lesions with ^{18}F-PSMA-1007 was shown ($P = 0.024$) at the expense of the interpretability of skeletal lesions. ^{18}F-PSMA-1007 showed significantly ($P = 0.0006$) more aspecific medullary focal uptake. However, in another study, which included 12 patients scanned with both ^{18}F-DCFPyL and ^{18}F-PSMA-1007, both radiopharmaceuticals identified the same lesions; the appearance of equivocal skeletal uptake was not mentioned (*15*).

Recently, Rauscher et al. performed a matched-pair analysis of ^{68}Ga-PSMA-11 and ^{18}F-PSMA-1007 and found an almost 5 times higher prevalence of PSMA-ligand–positive findings attributed to a benign origin, including among other bone lesions and lymph nodes (*21*). In this study, as in our present study, the lack of histopathologic confirmation represents a major limitation. To our knowledge, ours was the first study comprising a large cohort of patients assessing the differences between 2 widely used ^{18}F-PSMA radiopharmaceuticals.

Nonspecific skeletal ^{18}F-PSMA-1007 uptake has an unknown mechanism and shows great heterogeneity between patients (Fig. 1). It might be hypothesized that radiolysis results in free ^{18}F-fluorine; however, quality control reports from our cyclotron facility mention concentrations of free ^{18}F-fluorine below 2% at 8 h after synthesis of ^{18}F-PSMA-1007. Furthermore, the aspecific skeletal uptake was not seen in patients whose prostate cancer was scanned with ^{18}F-sodium fluoride (*22*). Therefore, it is unlikely that the uptake is explained by the presence of free ^{18}F-fluorine due to radiolysis. The literature comparing PSMA tracers with ^{68}Ga and ^{18}F has suggested that the higher number of equivocal lesions found with ^{18}F-PSMA-1007 might be explained by the lower positron energy (which improves spatial resolution), longer half-life, and generally higher injected activities of ^{18}F than of ^{68}Ga (*21*). However, since this study compared 2 different ^{18}F-labeled PSMA tracers, it can be concluded that the differences in physical properties of ^{68}Ga and ^{18}F do not offer a good explanation for the number of equivocal lesions found with ^{18}F-PSMA-1007. It is known that PSMA uptake may appear in several benign (bone) lesions (*23*); therefore, one hypothesis is that higher affinity of ^{18}F-PSMA-1007 for the PSMA receptor, as shown in preclinical studies, may result in a higher signal from these benign lesions (*24*). Another possibility is that ^{18}F-PSMA-1007 is metabolized (e.g., in the liver before excretion in the bile), resulting in radiolabeled substances that accumulate at specific sites in the skeleton, although there is no scientific underpinning for this hypothesis.

Given the findings in the present study and in the available literature, it can be concluded that there are differences between ^{18}F-DCFPyL and ^{18}F-PSMA-1007 that may have clinical consequences. Although there are clues that ^{18}F-DCFPyL may be more appropriate when information about uptake in the prostate is of no clinical value (e.g., in primary staging of prostate cancer that is already histopathologically proven), and although ^{18}F-PSMA-1007 may be more appropriate when detection of abnormalities in the prostate or prostatic fossa are most clinically relevant, there is too little evidence to support recommendations on which tracer should be used. Further studies are needed to verify the clues found in this study and in the available literature, especially studies to analyze the true nature of the equivocal bone lesions frequently found with ^{18}F-PSMA-1007 and the apparent better ability of ^{18}F-PSMA-1007 to detect lesions in the prostate and prostatic region.

CONCLUSION

Great equality was found between ^{18}F-DCFPyL and ^{18}F-PSMA-1007; however, some differences were observed that may be of clinical relevance. ^{18}F-PSMA-1007 detected prostatic lesions and prostatic fossa lesions in a higher proportion of patients, whereas ^{18}F-DCFPyL showed fewer equivocal skeletal lesions and higher interreader agreement for skeletal lesions. These differences encourage further studies to evaluate their true clinical impact, as they may have consequences for selection of the proper PSMA-targeting radiopharmaceutical.

DISCLOSURE

No potential conflict of interest relevant to this article was reported.

KEY POINTS

QUESTION: Are differences in the biologic behavior of different PSMA tracers clinically relevant to interreader agreement and to the detection rate for suspected malignant lesions?

PERTINENT FINDINGS: Interreader agreement was generally better for ^{18}F-DCFPyL than for ^{18}F-PSMA-1007, particularly regarding bone lesions. A statistically greater number of suspected lesions was found in the prostate or prostatic fossa with ^{18}F-PSMA-1007, especially in the biochemical-recurrence subcohort (P = 0.007–0.029), whereas ^{18}F-DCFPyL found a statistically lower number of equivocal bone lesions, particularly in the biochemical-recurrence (P = 0.003–0.013) and primary-staging (P = 0.001–0.065) cohorts

IMPLICATIONS FOR PATIENT CARE: Although more studies are needed to further explore the exact clinical implications of the present findings, these findings may allow for better selection of PSMA-targeted radiopharmaceuticals and therefore increase the diagnostic power of PSMA PET/CT.

REFERENCES

1. Afshar-Oromieh A, Zechmann CM, Malcher A, et al. Comparison of PET imaging with a ^{68}Ga-labelled PSMA ligand and ^{18}F-choline-based PET/CT for the diagnosis of recurrent prostate cancer. *Eur J Nucl Med Mol Imaging.* 2014;41:11–20.
2. Bluemel C, Krebs M, Polat B, et al. ^{68}Ga-PSMA-PET/CT in patients with biochemical prostate cancer recurrence and negative ^{18}F-choline-PET/CT. *Clin Nucl Med.* 2016;41:515–521.
3. Corfield J, Perera M, Bolton D, Lawrentschuk N. ^{68}Ga-prostate specific membrane antigen (PSMA) positron emission tomography (PET) for primary staging of high-risk prostate cancer: a systematic review. *World J Urol.* 2018;36:519–527.
4. van Kalmthout LWM, van Melick HHE, Lavalaye J, et al. Prospective validation of gallium-68 PSMA-PET/CT in primary staging of prostate cancer patients. *J Urol.* 2020;203:537–545.

5. Gorin MA, Rowe SP, Patel HD, et al. Prostate specific membrane antigen targeted ^{18}F-DCFPyL positron emission tomography/computerized tomography for the preoperative staging of high risk prostate cancer: results of a prospective, phase II, single center study. *J Urol.* 2018;199:126–132.
6. Roach PJ, Francis R, Emmett L, et al. The impact of ^{68}Ga-PSMA PET/CT on management intent in prostate cancer: results of an Australian prospective multicenter study. *J Nucl Med.* 2018;59:82–88.
7. Calais J, Czernin J, Cao M, et al. ^{68}Ga-PSMA-11 PET/CT mapping of prostate cancer biochemical recurrence after radical prostatectomy in 270 patients with a PSA level of less than 1.0 ng/mL: impact on salvage radiotherapy planning. *J Nucl Med.* 2018;59:230–237.
8. Ost P, Reynders D, Decaestecker K, et al. Surveillance or metastasis-directed therapy for oligometastatic prostate cancer recurrence: a prospective, randomized, multicenter phase II trial. *J Clin Oncol.* 2018;36:446–453.
9. Eiber M, Fendler WP, Rowe SP, et al. Prostate-specific membrane antigen ligands for imaging and therapy. *J Nucl Med.* 2017;58(suppl):67S–76S.
10. Szabo Z, Mena E, Rowe SP, et al. Initial evaluation of [^{18}F]DCFPyL for prostate-specific membrane antigen (PSMA)-targeted PET imaging of prostate cancer. *Mol Imaging Biol.* 2015;17:565–574.
11. Afshar-Oromieh A, Malcher A, Eder M, et al. PET imaging with a [^{68}Ga]gallium-labelled PSMA ligand for the diagnosis of prostate cancer: biodistribution in humans and first evaluation of tumour lesions. *Eur J Nucl Med Mol Imaging.* 2013;40:486–495.
12. Herrmann K, Bluemel C, Weineisen M, et al. Biodistribution and radiation dosimetry for a probe targeting prostate-specific membrane antigen for imaging and therapy. *J Nucl Med.* 2015;56:855–861.
13. Afshar-Oromieh A, Hetzheim H, Kratochwil C, et al. The theranostic PSMA ligand PSMA-617 in the diagnosis of prostate cancer by PET/CT: biodistribution in humans, radiation dosimetry, and first evaluation of tumor lesions. *J Nucl Med.* 2015;56:1697–1705.
14. Afshar-Oromieh A, Hetzheim H, Kubler W, et al. Radiation dosimetry of ^{68}Ga-PSMA-11 (HBED-CC) and preliminary evaluation of optimal imaging timing. *Eur J Nucl Med Mol Imaging.* 2016;43:1611–1620.
15. Giesel FL, Will L, Lawal I, et al. Intraindividual comparison of ^{18}F-PSMA-1007 and ^{18}F-DCFPyL PET/CT in the prospective evaluation of patients with newly diagnosed prostate carcinoma: a pilot study. *J Nucl Med.* 2018;59:1076–1080.
16. Giesel FL, Hadaschik B, Cardinale J, et al. F-18 labelled ^{18}F-PSMA-1007: biodistribution, radiation dosimetry and histopathological validation of tumor lesions in prostate cancer patients. *Eur J Nucl Med Mol Imaging.* 2017;44:678–688.
17. Rowe SP, Pienta KJ, Pomper MG, Gorin MA. PSMA-RADS version 1.0: a step towards standardizing the interpretation and reporting of PSMA-targeted PET imaging studies. *Eur Urol.* 2018;73:485–487.
18. Landis JR, Koch GG. The measurement of observer agreement for categorical data. *Biometrics.* 1977;33:159–174.
19. Wondergem M, Jansen BHE, van der Zant FM, et al. Early lesion detection with ^{18}F-DCFPyL PET/CT in 248 patients with biochemically recurrent prostate cancer. *Eur J Nucl Med Mol Imaging.* 2019;46:1911–1918.
20. Dietlein F, Kobe C, Hohberg M, et al. Intraindividual comparison of ^{18}F-PSMA-1007 with renally excreted PSMA ligands for PSMA PET imaging in patients with relapsed prostate cancer. *J Nucl Med.* 2020;61:729–734.
21. Rauscher I, Krönke M, König M, et al. Matched-pair comparison of ^{68}Ga-PSMA-11 PET/CT and ^{18}F-PSMA-1007 PET/CT: frequency of pitfalls and detection efficacy in biochemical recurrence after radical prostatectomy. *J Nucl Med.* 2020;61:51–57.
22. Wondergem M, van der Zant FM, Knol RJJ, et al. ^{99m}Tc-HDP bone scintigraphy and ^{18}F-sodiumfluoride PET/CT in primary staging of patients with prostate cancer. *World J Urol.* 2018;36:27–34.
23. Sheikhbahaei S, Afshar-Oromieh A, Eiber M, et al. Pearls and pitfalls in clinical interpretation of prostate-specific membrane antigen (PSMA)-targeted PET imaging. *Eur J Nucl Med Mol Imaging.* 2017;44:2117–2136.
24. Cardinale J, Schäfer M, Benešová M, et al. Preclinical evaluation of ^{18}F-PSMA-1007, a new prostate-specific membrane antigen ligand for prostate cancer imaging. *J Nucl Med.* 2017;58:425–431.